Environmental Science & Technology

pubs.acs.org/est

Article

Maternal $PM_{2.5}$ Exposure and Cardiac Developmental Abnormalities in Fetuses and Neonates: Progressive Activation of the Complement and Coagulation Cascade

Yuqiong Guo, Sican Niu, Yingying Zhang, Wei Yan, Shaoyang Ji, Li Ma, Guangke Li,* and Nan Sang*

Cite This: https://doi.org/10.1021/acs.est.4c11407

Read Online

ACCESS | Metrics & More | Article Recommendations | Supporting Information

ABSTRACT: Emerging studies indicate a positive correlation between maternal $PM_{2.5}$ exposure and an increased risk of congenital heart diseases (CHDs). However, the developmental origins in fetal and neonatal offspring, as well as the underlying mechanisms, remain elusive. To bridge this gap, we established an animal model of maternal $PM_{2.5}$ exposure and confirmed its adverse effects on cardiac function and structure in neonates, primarily left ventricular systolic and diastolic dysfunction and myocardial hypertrophy in both male and female offspring, characterized by thick ventricular walls and narrowed ventricular chambers at embryonic (E) day 18.5. Then, combining transcriptional profiling and immunohistochemical analyses, we found that the upregulation of myosin-related genes was a key mediator in these myocardial contraction abnormalities. Importantly, using time-series transcriptome analysis across critical windows of cardiac development (E10.5, E14.5, and E18.5), we uncovered that the complement and coagulation cascade signaling pathways were progressively activated, triggering cellular inflammation and lysis and upregulating myosin genes, which ultimately contributed to compensatory cardiac hypertrophy and cardiac dysfunction. This work provides a comprehensive perspective for local governments and clinicians to control and prevent CHD burden in polluted areas.

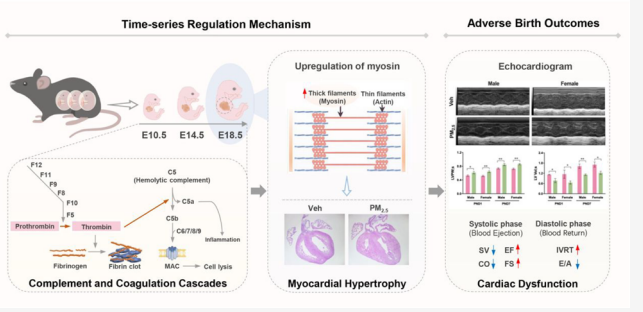

KEYWORDS: *maternal $PM_{2.5}$ exposure, cardiac development, myocardial hypertrophy, complement and coagulation cascade, myosin-related genes*

1. INTRODUCTION

Congenital heart disease (CHD) includes structural anomaly of the heart and great vessels present at birth,[1] often characterized by specific hemodynamic issues such as volume and pressure overload, pulmonary hypertension and cyanosis, which can progress to cardiac hypertrophy and cardiac cell damage and death.[2] Affecting approximately 1% of live-born infants[3] and accounting for more than 40% of prenatal deaths,[4] CHD represents a significant global health challenge.[5] In addition to maternal factors, such as obesity and diabetes, smoking in pregnancy, medicine usage, and contact with organic solvents,[6] more and more epidemiological studies indicate that maternal exposure to air pollutants, especially fine particulate matter ($PM_{2.5}$), significantly contributes to CHD risks in offspring.[4,7,8]

A cohort study in Canada comprising 1,342,198 newborns, of whom 12,715 suffer from heart defects, demonstrated that $PM_{2.5}$ exposure in early pregnancy is associated with an increased risk of heart defects, particularly atrial septal defects (with an association of 1.08 (95% CI: 1.03, 1.14)).[9] In a nationwide surveillance-based case-control study of China, maternal $PM_{2.5}$ exposure, especially in the preconception period, is linearly correlated to the total incidence of CHDs and specific CHD types in offspring, with septal defects being the most prevalent subtype.[10] Using the Bayesian multinomial probit model for jointly identifying daily windows of susceptibility for 12 types of CHDs related to maternal $PM_{2.5}$ exposure, an association is observed between increased $PM_{2.5}$ exposure and the progression of pulmonary valvular stenosis on postnatal day (PND) 53, as well as tetralogy of Fallot on PND50−51.[11] Given that only up to 15% of CHD cases have a determined genetic etiology,[4] exploring the interaction between environmental factors (including ambient $PM_{2.5}$ exposure) and genetic variations can provide novel insights to CHD pathogenesis.

CHD results from the perturbation of normal cardiac development.[12] The heart, one of the earliest developing organs during embryogenesis, undergoes a complex process

Received: October 21, 2024
Revised: July 18, 2025
Accepted: July 21, 2025

that requires interactions among multiple cell types and is governed by specific spatial and temporal rules,[13] including the appearance of cardiac tubes, the formation of the atrioventricular septum, the establishment of the circulatory system, the proliferation and differentiation of myocardial cells, and the development of valves.[14,15] Animal studies demonstrate that maternal exposure to $PM_{2.5}$ during pregnancy led to cardiac dysfunction, including heart failure and electrical remodeling in offspring during puberty and adulthood.[16,17] However, due to the presence of sensitive windows and spatiotemporal dynamics in cardiac development, current epidemiological studies are limited to correlation analyses, failing to clarify the causality between maternal $PM_{2.5}$ exposure and CHDs. Moreover, cardiac development is a dynamic process, and focusing on a single time point is insufficient to elucidate the mechanisms underlying the causal relationship between $PM_{2.5}$ and CHDs.

In the present study, we established a maternal $PM_{2.5}$ exposure model, and aimed to (1) confirm cardiac functional and structural abnormalities in fetal/neonatal offspring; (2) clarify the toxicological characteristics at developmental windows in the fetus; (3) uncover potential time-series regulatory mechanisms for abnormal heart development. This study would like to provide novel insights into CHD risk in $PM_{2.5}$-polluted areas and find potential targets for controlling and preventing children from disease burdens.

2. MATERIALS AND METHODS

2.1. $PM_{2.5}$ Collection. $PM_{2.5}$ samples were collected in Taiyuan, Shanxi Province from November 2018 to February 2019, which corresponds to the heating period in northern China. The samples were collected using quartz filters (F90 mm, Sweden) on a PM middle-volume air sampler (22 h/day, with a 100 L/min flow rate, TH-100CIII, China). Then, the blank and $PM_{2.5}$ filters were immersed in Milli-Q water and sonicated for the preparation of vehicle and exposure solutions, respectively. The suspension was filtered and freeze-dried as previously reported.[18] $PM_{2.5}$ has been characterized in our previous work.[19]

2.2. Animals and Maternal $PM_{2.5}$ Exposure. Male and female C57BL/6 mice were obtained from Beijing Vital River Laboratory Animal Technology (Beijing, China) and housed under standard conditions (22.11 ± 1.51 °C), with free access to food and water. After acclimatization for 1 week, 80 female mice were mated with 80 male mice (one female and one male per cage), and plug-positive female mice were considered pregnant.[20] Pregnant mice were exposed to either $PM_{2.5}$ suspensions (3 mg/kg) or vehicle via oropharyngeal aspiration every 2 days for the entire pregnancy period, as described in our previous study.[18] Offspring were euthanized on embryonic days 10.5, 14.5, and 18.5 (E10.5, E14.5, and E18.5) and PND1 and PND7. Cardiac tissues were dissected for further analysis, and one male or female offspring per litter was used in each experiment. All animal experiments were approved by the Committee of Scientific Research at Shanxi University.

2.3. Echocardiography. To assess the cardiac function of offspring after maternal $PM_{2.5}$ exposure, mice were subjected to echocardiography at PND1 and PND7, including the left ventricular (LV) function and structure, using a Vevo 2100 imaging system (FUJIFILM VisualSonics). The detailed procedure has been described previously.[21] All tests were performed on 6−10 pups/group, which were randomly selected from 3 dams.

2.4. Morphological Observation. Dams were sacrificed at E10.5, E14.5, and E18.5 to obtain embryos, and fetal hearts were dissected in precooled PBS. The harvested heart was placed in clean precooled PBS and photographed using an Asana microscope (Olympus).

2.5. Histopathological Observation. Three fetal cardiac tissues were randomly selected from each group for H&E and wheat germ agglutinin (WGA) stainings, which were performed by Servicebio Technology Co., Ltd. (Wuhan, China), and the detailed procedure was described in the Appendix A in Supporting Information.

2.6. Quantitative Real-Time PCR. Total RNA was extracted from fetal cardiac tissues at E10.5, E14.5, and E18.5 using Trizol (Invitrogen) and quantified using a Nanodrop spectrophotometer (Thermo Fisher Scientific). The cDNA was synthesized using a Reverse Transcription Kit (Takara, China). Finally, gene expression levels were determined using RT-qPCR (TaKaRa, China) with Gapdh as an internal reference gene. The sequences of gene-specific primers are listed in Table S1.

2.7. Transcriptomics. Fetal cardiac tissues (30 mg) at E10.5, E14.5, and E18.5 from each group were used for transcriptomics performed by Shanghai Biotechnology Corporation (Shanghai, China). Total RNA was extracted with TRIzol reagent (Invitrogen) and purified with a RNeasy Mini reagent kit (Qiagen). And then RNA was subsequently used for fluorescently labeling cDNA targets (made by Agilent Technologies). The labeled cDNA targets were scanned on an Agilent Microarray Scanner, and data were extracted and normalized using quantum algorithms in Feature Extraction version 11 (Agilent technologies). Differentially expressed genes (DEGs) were identified based on p-value < 0.05 and $|\text{fold-change}| \geq 2$. The Gene Ontology (GO) terms and Kyoto Encyclopedia of Genes and Genomes (KEGG) pathway enrichment of DEGs were analyzed using DAVID (https://david.ncifcrf.gov/home.jsp), and the relationship between DEGs and cardiovascular disease was predicted using the Comparative Toxicogenomics Database (CTD, https://comptox.epa.gov/dashboard/).

2.8. Immunohistochemical Staining (IHC). Cardiac sections were deparaffinized with xylene, rehydrated with gradient ethanol, and treated with citrate buffer for antigen retrieval. The sections were blocked with 3% BSA for 30 min and incubated with Anti-Fast Myosin Skeletal Heavy chain pAb (1:200 dilution, Servicebio, Wuhan, China), Anti-FGG pAb (1:200 dilution, Proteintech, Wuhan, China), Anti-C5 pAb (1:100 dilution, Beyotime Biotechnology, Shanghai, China) and Anti-F12 pAb (1:200 dilution, Proteintech, Wuhan, China) overnight. After washing with PBS, the sections were incubated with the enzyme-labeled goat antirabbit IgG (1:200 dilution, Servicebio, Wuhan, China) at room temperature for 30 min. After washing with PBS, the sections were stained with DAB for 5 min. Finally, the sections were dehydrated, cleared, sealed with neutral resin, and observed under a light microscope.

2.9. Enzyme-Linked Immunosorbent Assay (ELISA). Approximately 20 mg of cardiac tissue was homogenized in 180 μL of sterile saline, followed by centrifugation to collect the supernatant. Then, the level of the membrane attack complex (MAC) in the supernatant was measured using ELISA kits (Saipeisen Biology, Shanghai, China) according to the manufacturer's instruction.

https://doi.org/10.1021/acs.est.4c11407
Environ. Sci. Technol. XXXX, XXX, XXX−XXX

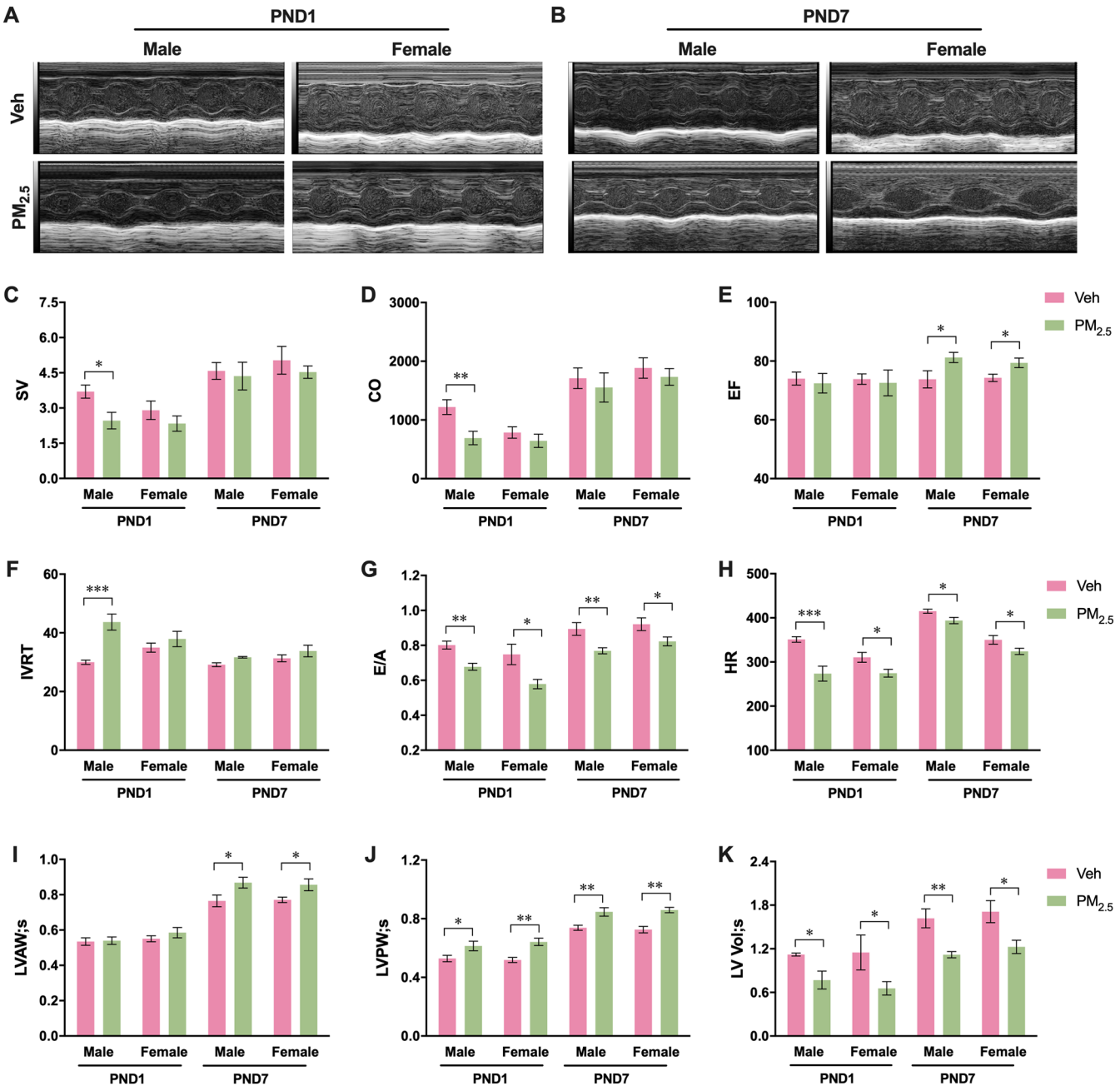

Figure 1. Cardiac function and structural alterations in PND1 and PND7 offspring after maternal $PM_{2.5}$ exposure. (A, B) Representative images of echocardiography. (C−E) Effects on cardiac systolic function, including SV (stroke volume), CO (cardiac output), and EF (ejection fraction). (F, G) Effects on cardiac diastolic function, including IVRT (isovolumic relaxation time) and E/A (Early diastolic filling velocity to Atrial filling velocity ratio). (H) Effects on HR (heart rate). (I−K) Effects on cardiac structure, including LVAW;s (systolic left ventricular anterior wall thickness), LVPW;s (left ventricular end-systolic posterior wall thickness), and LV Vol;s (systolic left ventricular volume). Data are expressed as means ± SEM (n = 6−8); *p < 0.05, **p < 0.01, ***p < 0.001 versus the vehicle control.

2.10. Thrombin Inhibitor Treatment. Pregnant mice were divided into three groups and treated accordingly once every 2 days until E18.5 ceased, including the vehicle control group (oropharyngeal aspiration with vehicle, subcutaneous injection with saline), the $PM_{2.5}$-exposed group (oropharyngeal aspiration with $PM_{2.5}$ suspension, subcutaneous injection with saline), and the inhibitor group (oropharyngeal aspiration with $PM_{2.5}$ suspensions, subcutaneous injection of recombinant hirudin). Recombinant hirudin was purchased from Macklin (Shanghai, China). The inhibitor group was subcutaneously injected with 2 U of recombinant hirudin (dissolved in 300 μL of saline) each time, and the remaining groups were subcutaneously injected with an equal volume of saline.

2.11. Statistical Analyses. Data were analyzed with GraphPad Prism software, and the results were expressed as the mean ± standard error (SEM). Comparisons between two groups were performed using a Two-tailed Student's t test, and unequal variances were corrected using Welch's method. p < 0.05 was considered statistically significant. Some of the image materials sourced from Figdraw (licensed) (https://www.figdraw.com/static/index.html#/).

https://doi.org/10.1021/acs.est.4c11407
Environ. Sci. Technol. XXXX, XXX, XXX−XXX

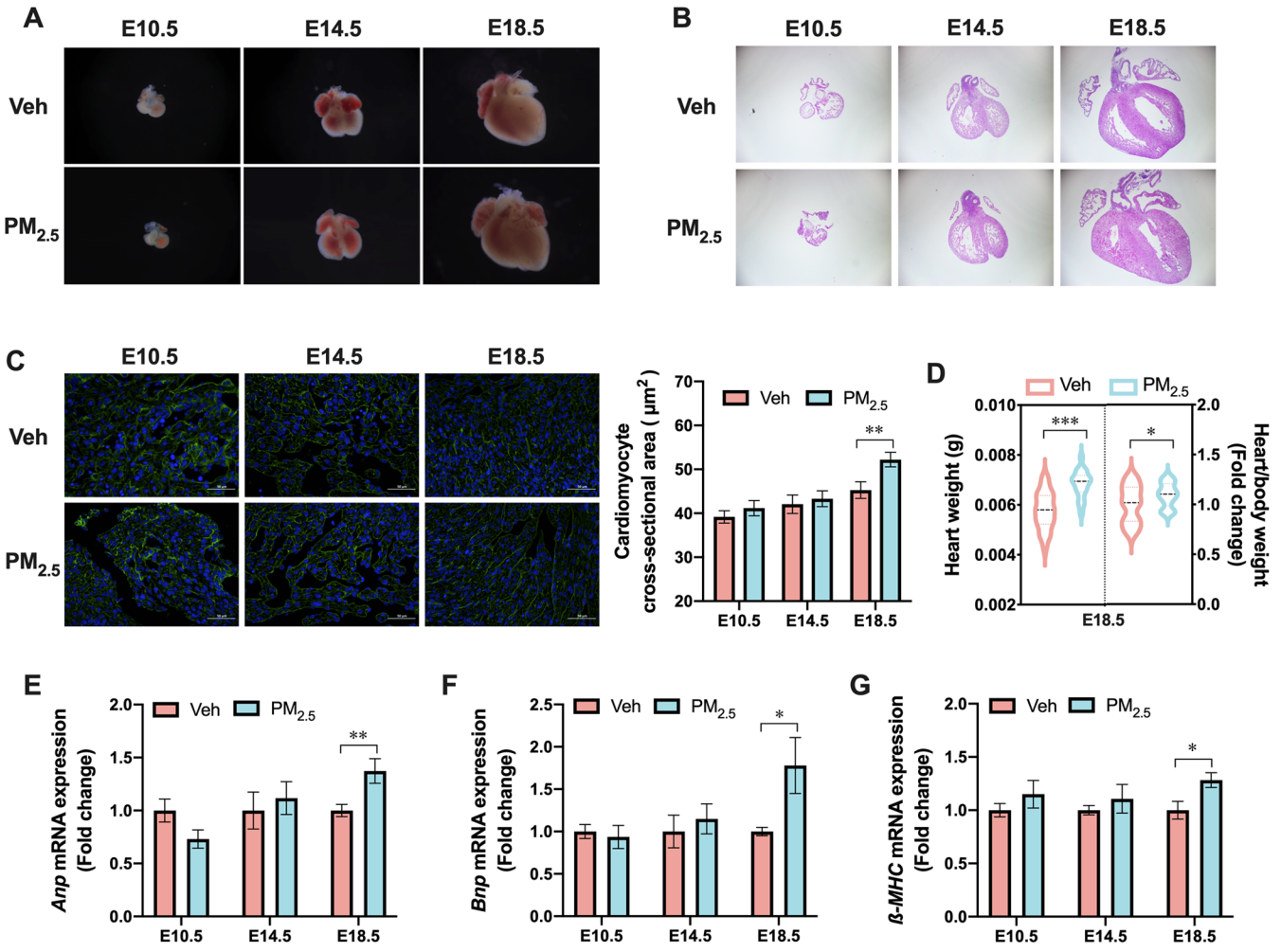

Figure 2. Cardiac morphological and histological alterations in E10.5, E14.5, and E18.5 embryos following maternal $PM_{2.5}$ exposure. (A) Representative images of fetal hearts at E10.5, E14.5, and E18.5. (B) Representative images of H&E-stained cardiac sections at E10.5, E14.5, and E18.5. (C) Representative images of FITC-conjugated WGA-stained cardiac tissues (scale bars representing 50 mm) (left) and the effects on the cardiomyocyte cross-sectional area in cardiac tissues ($n = 3$) (right). (D) Heart weights and heart/body weights ($n = 21-24$) of embryos at E18.5. (E-G) The mRNA expression of *Anp*, *Bnp*, and *β-MHC* ($n = 6-10$). Data are expressed as means ± SEM ($n = 6-8$); $^*p < 0.05$, $^{**}p < 0.01$, $^{***}p < 0.001$ versus the vehicle control.

3. RESULTS AND DISCUSSION

Maternal $PM_{2.5}$ exposure has been linked to abnormal cardiac development and an increased risk of CHDs.[22−24] However, limited animal experiments primarily focused on disease susceptibility and postnatal developmental alterations, it remains largely unknown about the causal relationship and mechanisms underlying abnormal structural and functional development in both neonatal and embryonic hearts.

3.1. Alterations in Cardiac Structure and Function in Neonatal Offspring. Echocardiography is commonly used to characterize the mouse cardiac function and morphology in both clinical and preclinical studies.[25] Here, it was used to assess ventricular systolic and diastolic capacity, ventricular chamber size, and ventricular wall thickness in offspring at PND1 and PND7 (Figure 1A,B) following maternal $PM_{2.5}$ exposure. For the LV systolic function, the IVCT (isovolumetric contraction time) showed no significant changes (Figure S1A), whereas the SV (stroke volume) and CO (cardiac output) significantly decreased in male mice at PND1, and similar trends were also observed in females (Figure 1C,D). However, the EF (ejection fraction) and FS (left ventricular short axis shortening rate) were markedly elevated in both male and female mice at PND7 (Figures 1E and S1B), possibly a compensatory response to reduced end-diastolic volume following the exposure.[26] For the LV diastolic function, the IVRT (isovolumic relaxation time) was prolonged and the E/A (Early diastolic filling velocity to Atrial filling velocity ratio) dramatically decreased in both male and female offspring at PND1 and PND7 (Figure 1F,G), suggesting that maternal $PM_{2.5}$ exposure decreased myocardial diastolic function in offspring. In addition, we observed a persistent decreased heart rate at PND1 and PND7 (Figure 1H), which might be attributed to intrauterine distress or abnormal cardiac structure following maternal $PM_{2.5}$ exposure.[27]

Cardiac dysfunction is often coupled with structural remodeling.[28] Therefore, we further determined the parameters of the LV structure. For the LV wall, the LVAW;s (systolic left ventricular anterior wall thickness) significantly increased at PND7 (Figure 1I), with no obvious changes observed in LVAW;d (diastolic left ventricular anterior wall thickness) (Figure S1C). In comparison, both LVPW;s (left ventricular end-systolic posterior wall thickness) and LVPW;d (left ventricular end-diastolic posterior wall thickness) remarkably

https://doi.org/10.1021/acs.est.4c11407
Environ. Sci. Technol. XXXX, XXX, XXX−XXX

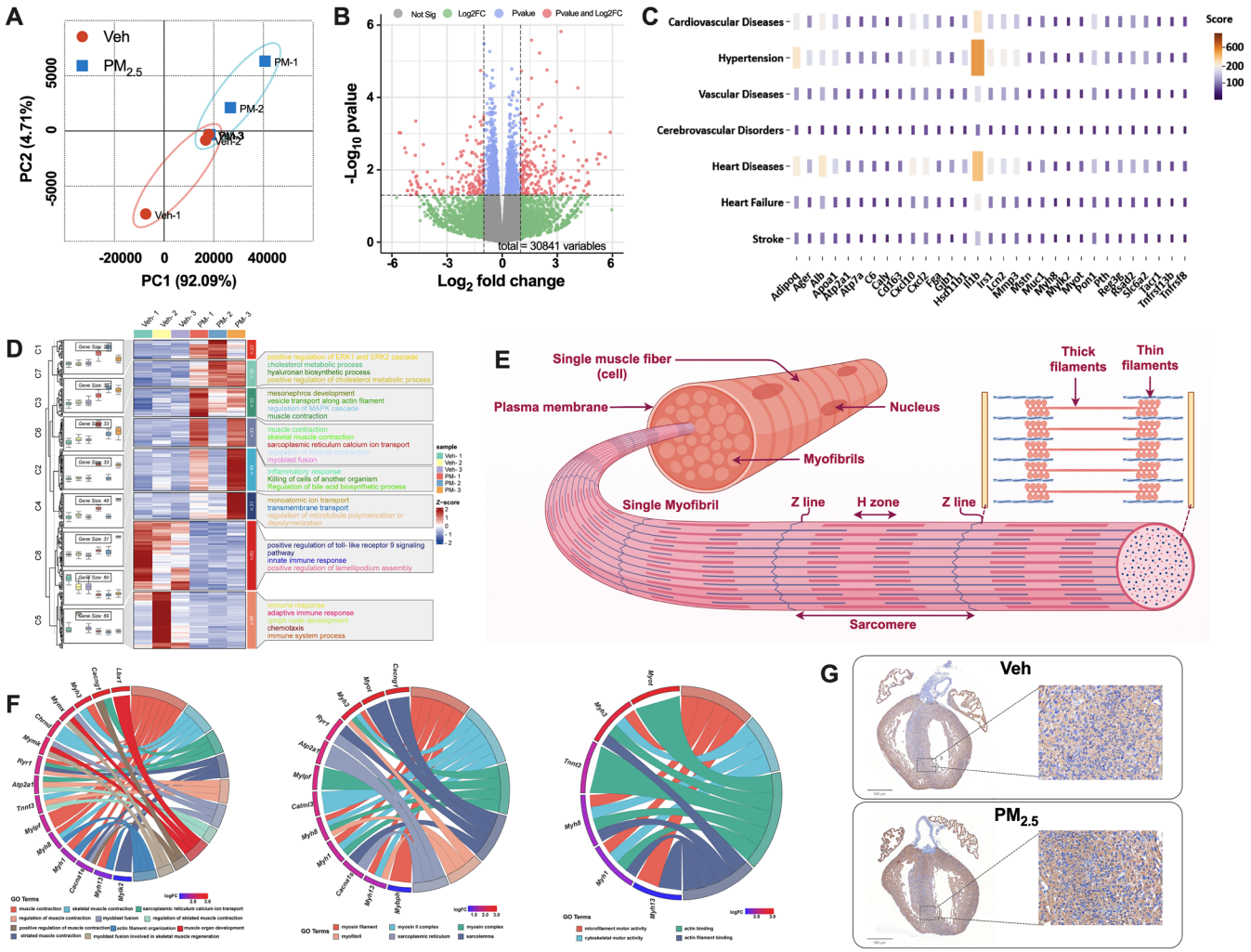

Figure 3. Transcriptional expression profile of fetal hearts at E18.5 following maternal $PM_{2.5}$ exposure. (A) Principal component analysis (PCA) map in the $PM_{2.5}$-exposed and vehicle control groups. (B) Volcano plot showing the expression of DEGs. (C) Gene-disease enrichment analysis showing the relationship between target genes and predicted diseases in CTD. The color and size of the blocks represent inference scores between predicted diseases and target genes. (D) Trend clustering annotated heatmap. C1−C8 represent subgroups clustered according to the gene expression values of different samples. (E) Schematic diagram of myocardial fiber structure. (F) String plot representing the relationship between DEGs and the enriched BP/CC/MF terms. (G) Representative IHC images of myosin skeletal heavy chain.

increased at both PND1 and PND7 (Figures 1J and S1D), suggesting that maternal $PM_{2.5}$ exposure triggered neonatal myocardial hypertrophy, predominantly affecting the LV posterior wall. For the LV cavity, we observed a notable decrease in LVID (left ventricular internal diameter) (Figure S1E,F), leading to a correspondingly smaller LV Vol (left ventricular volume), especially in the systolic phase (Figures 1K and S1G), and a slight increase in LV mass (Figure S1H).

These findings suggest that maternal $PM_{2.5}$ exposure caused myocardial hypertrophy and diastolic dysfunction in offspring. Myocardial maturation relies on a balance between cell hypertrophy and hyperplasia with cell proliferation predominating during the embryonic stage and cell hypertrophy progressively dominating to increase cardiomyocyte size during postnatal transition.[29,30] However, throughout the life course, to counteract pathologies such as hemodynamic abnormalities and pressure overload caused by environmental pollution, cardiac hypertrophy activated by the renin-angiotensin-aldosterone (RAA) system can serve as a compensatory mechanism to maintain cardiac function.[2,31] Similarly, Vineeta et al. found that intrauterine $PM_{2.5}$ exposure led to a substantial increase in the thickness of the LV posterior wall and developed concentric hypertrophy in mice.[16] In addition, prenatal diesel exhaust exposure resulted in cardiac hypertrophy and fibrosis in adult offspring following transverse aortic constriction,[32] which was consistent with our results.

3.2. Abnormal Cardiac Structural Development and Myocardial Hypertrophy in Fetuses. Childhood diseases can often be attributed to perturbations in fetal development resulting from exposure to environmental pollutants during early life.[33] To clarify the possible developmental origin for structural and functional alterations in neonatal offspring following maternal $PM_{2.5}$ exposure and identify the critical window, we analyzed the growth parameters and pathological characteristics of the heart in embryos/fetuses at several time points (E10.5, E14.5, and E18.5). As illustrated in Figure 2A, at E10.5, the fetuses in both vehicle control and $PM_{2.5}$-exposed groups exhibited visible atrioventricular and valvular structures as well as great-vessel connections, suggesting the preliminary formation of the cardiac circulatory system. At E14.5, the heart becomes mature and begins to function following cardiomyocyte proliferation and differentiation, valve development, and

https://doi.org/10.1021/acs.est.4c11407
Environ. Sci. Technol. XXXX, XXX, XXX−XXX

cardiac conduction system formation. At this stage, maternal $PM_{2.5}$ exposure did not notably affect cardiac morphology or voluntary beating. However, as the heart progressively grows to meet the demands of upcoming postnatal life, notable changes were observed at E18.5. H&E staining revealed ventricular wall thickening, irregular arrangement of cardiomyocytes, and narrowed ventricular chambers (Figure 2B), indicating the onset of concentric myocardial hypertrophy, which was in line with the echocardiographic findings in offspring previously described. Meanwhile, WGA staining showed that the cross-sectional area (CSA) of cardiomyocytes in the $PM_{2.5}$-exposed group was significantly larger than those in vehicle controls (Figure 2C). Consistently, the heart weight and heart-to-body weight ratio also increased dramatically (Figure 2D).

Biomarker measures facilitate the validation of these pathological alterations and provide information about processes such as contractile stress and ventricular remodeling.[2,34] β-myosin heavy chain (β-MHC) is a common regulator linked to cardiac hypertrophy and exhibits specific expression in mammalian hearts.[35,36] Additionally, atrial natriuretic peptide (ANP) and B-type natriuretic peptide (BNP) are synthesized within cardiomyocytes and subsequently released into the circulatory system upon exposure to pathological stimuli, thereby resulting in structural anomalies and cardiac dysfunction.[37,38] Here, we examined the mRNA expression of *β-MHC*, *Anp* and *Bnp*, and found that their expressions were significantly up-regulated in the exposed mice at E18.5, with no meaningful alterations at E10.5 and E14.5 (Figure 2E−G). Together, these results suggest that maternal $PM_{2.5}$ exposure induced cardiac dysfunction and structural remodeling, deriving from an imbalance between proliferation and hypertrophy of late-gestational cardiomyocytes.

3.3. Myosin-Related Gene Expression in Response to Myocardial Hypertrophy. To further explore the potential regulation of myocardial hypertrophy in offspring, we first analyzed the transcriptional profile of fetal hearts at E18.5. The overall gene expression distribution of each RNA-seq sample is presented in Figure S2A. The PCA model indicated that maternal $PM_{2.5}$ exposure caused obvious alterations in the transcriptome in fetal hearts (Figure 3A). With the criterion of Log2 |foldchange| > 1 and $p < 0.05$, we identified a total of 344 DEGs, of which 198 were up-regulated and 146 were down-regulated (Figure 3B). Next, we analyzed the association of these DEGs with diseases using the CTD database and found that 31 DEGs were highly linked to cardiovascular diseases (Figure 3C), with hypertension sharing the highest overall inference score (Figure S2B), indicating excessive cardiac load in $PM_{2.5}$-exposed fetuses that triggered cardiac hypertrophy.[39] To evaluate the biological functions of DEGs, we clustered them according to the expression values of each sample and obtained eight clusters and their functional annotations (C1−C8), among which C1, C2, C3, C4, C6, and C7 were significantly up-regulated following maternal $PM_{2.5}$ exposure, while C5 and C8 were significantly down-regulated (Figure 3D). It is worth noting that C3 and C6 were enriched in a large number of terms related to myocardial dysfunction, including *muscle contraction*, *skeletal muscle contraction*, *sarcoplasmic reticulum calcium ion transport*, and *myoblast fusion* (Figure 3D), which was consistent with the results of cardiac echocardiography in offspring, especially the increased EF and FS. Similar to our results, Luo et al. found a large number of mutations in genes regulating early embryonic cardiac contractility, which was considered an important mechanism of CHD.[5]

Cardiac contraction is driven by the sliding filament mechanism within myocardial cells. When cardiomyocytes are depolarized, calcium ions (Ca^{2+}) are released from the sarcoplasmic reticulum (SR) into the cytoplasm, where they bind to cardiac troponin, leading to a conformational change in the troponin-myosin complex that facilitates the interaction between actin and myosin and generates cardiac contraction. Subsequently, calcium reuptake into the SR occurs, leading to cardiomyocyte diastole (Figure 3E).[40,41] Therefore, to clarify the structural basis of abnormal myocardial contraction, we analyzed the biological processes (BP), cellular components (CC) and molecular function (MF) of DEGs in C3 and C6, and found that myosin-related terms were significantly enriched, such as *myosin filament*, *myosin complex* and *myofibril* (Figure 3F). qPCR further validated the mRNA expression of myosin-associated DEGs in these terms, revealing that the levels of *Myh1*, *Myh8*, *Myh13*, *Mylk2*, and *Mylpf* were significantly up-regulated (Figure S3A). In addition, IHC staining showed a significant elevation of fast myosin skeletal heavy chain expression in the ventricular wall (Figures 3G and S3B).

Collectively, these results suggest that maternal $PM_{2.5}$ exposure elevated the expression of myosin genes in response to myocardial injury and hypertrophy during late pregnancy. The pattern of myosin work determines how the heart modulates force production, and an increased proportion of active myosin responds to higher energy expenditure during systole and diastole, promoting longer or stronger interactions with actin, ultimately contributing to diastolic dysfunction and hypercontractility.[42] During cardiac hypertrophy, to accommodate the augmented load, the heart may upregulate the expression of myosin genes to enhance myocardial contractility. This adaptive change may help maintain the pumping function of the heart in the short term, but it may further result in alterations in cardiac structure and function in the long term.[43] During the early stage of cardiac development, different isoforms of myosin begin to be expressed and differentiated, which can promote the proliferation, differentiation and migration of cardiomyocytes and lay the foundation for the formation of the basic structure of the heart.[44] However, during embryonic development, unfavorable factors may lead to abnormalities in myosin expression and function, such as the gradual replacement of some embryonic-type isoforms of myosin by adult-type ones, resulting in cardiac hypertrophy.[45,46] In contrast, myosin inhibitors, such as mavacamten, can act as a treatment for hypertrophic cardiomyopathy by blocking the binding of myosin to actin and thereby suppressing the generation of sarcomere force.[47] Importantly, even though a large body of literature has demonstrated a relationship between myosin and cardiac hypertrophy,[48−50] our study found that maternal $PM_{2.5}$ exposure caused myocardial hypertrophy in fetuses and neonates by altering myosin gene expression.

3.4. Complement and Coagulation Dysregulation for Abnormal Cardiac Development. During embryonic development, the formation and function of organs depend on the dynamic expression of specific genes at different time points.[51] To clarify the potential time-series regulatory mechanism associated with abnormal cardiac development in fetuses/neonates in response to maternal $PM_{2.5}$ exposure, we analyzed the transcriptional profiles of fetal hearts at three

https://doi.org/10.1021/acs.est.4c11407
Environ. Sci. Technol. XXXX, XXX, XXX−XXX

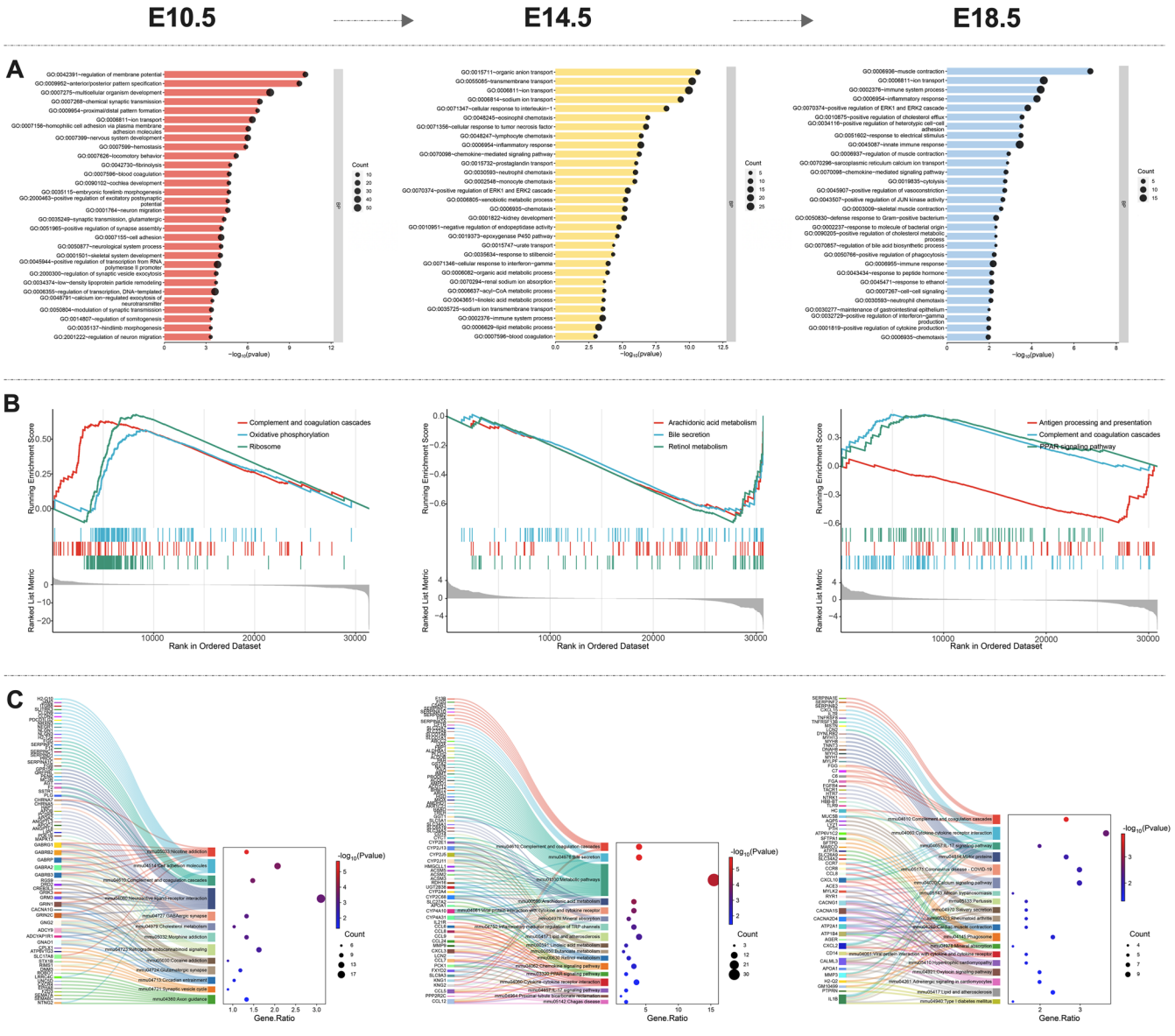

Figure 4. Transcriptional expression profile and biological processes in fetal hearts at E10.5, E14.5, and E18.5 following maternal $PM_{2.5}$ exposure. (A) Top 30 enriched BP terms of DEGs using DAVID analysis. Significantly enriched terms were screened when $p < 0.05$. (B) Top 3 GSEA results of all DEGs. Significantly enriched terms were screened based on $q < 0.05$ and |NES| > 1.5. (C) All enriched KEGG pathways of DEGs using DAVID analysis. Significantly enriched terms were screened when $p < 0.05$.

consecutive developmental windows E10.5, E14.5, and E18.5, yielding 799, 281, and 344 DEGs (Log2 |foldchange| > 1 and $p < 0.05$), respectively (Figure S4). By GO functional annotation, we found that among the top 30 BP terms, the DEGs at E10.5 were mainly enriched in neurological processes, such as *chemical synaptic transmission* (GO: 0007268) and *nervous system development* (GO: 0007399); DEGs at both E14.5 and E18.5 were significantly enriched in inflammation- and immune-related terms, such as *inflammatory response* (GO: 0006954), *immune system process* (GO: 0002376), and *chemotaxis* (GO: 0006935) (Figure 4A). Importantly, both gene set enrichment analysis (GSEA) and KEGG pathway annotation indicated the enrichment of *Complement and coagulation cascades* at three time points (Figure 4B,C). Complement and coagulation are two important biological systems and play a key role in maintaining the body's immune health and blood coagulation homeostasis.[52,53] In addition, there is extensive crosstalk between them and inflammation, and activation of one system may amplify activation of the other, which, if left unchecked, may lead to tissue damage and even multiorgan failure.[54] Here, the time-series transcriptomics suggest that complement and coagulation cascades acted as one of the key pathways for cardiac developmental abnormalities in offspring following maternal $PM_{2.5}$ exposure. Similarly, Jin et al. found that airborne fine particulate matter (PM) affected blood homeostasis by triggering crosstalk among the plasma kinin-releasing enzyme-kinin system (KKS), complement and coagulation systems.[55] Previous reports have shown that the coagulation and complement systems caused severe preeclampsia and affected cardiac development through various pathways, such as inflammation,

https://doi.org/10.1021/acs.est.4c11407
Environ. Sci. Technol. XXXX, XXX, XXX−XXX

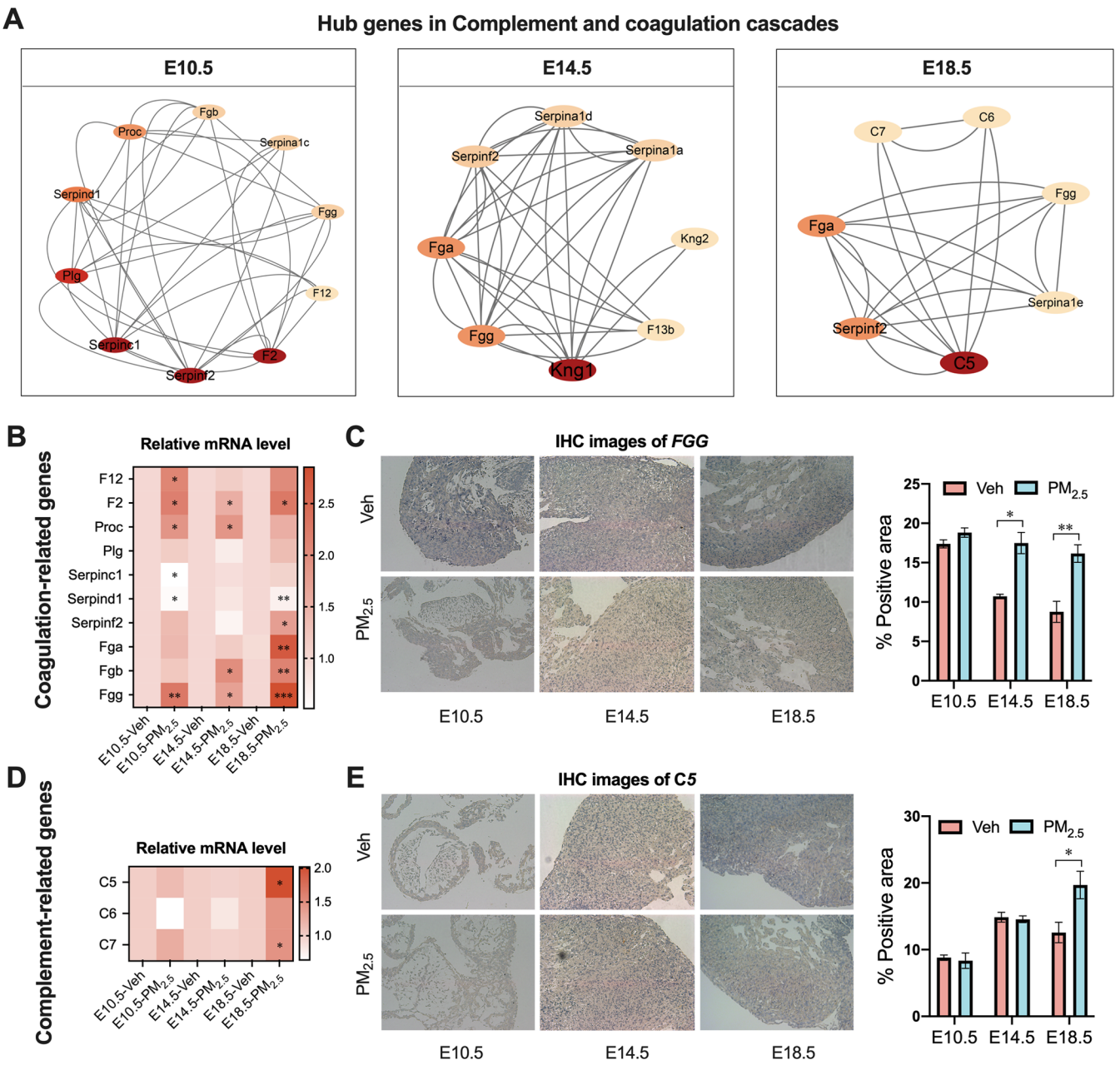

Figure 5. Persistent complement and coagulation dysregulation in fetal hearts following maternal $PM_{2.5}$ exposure. (A) Hub genes involved in the complement and coagulation cascade pathway determined by protein−protein interaction (PPI) network analysis at E10.5, E14.5, and E18.5. (B) The mRNA expression of the top 10 DEGs involved in the coagulation cascade (n = 6−10). (C) Representative IHC images of fetal hearts with anti-FGG at E10.5, E14.5, and E18.5 (Left), and the relative IOD of FGG (Right) (n = 4). (D) The mRNA expression of the 3 DEGs involved in the complement cascade (n = 6−10). (E) Representative IHC images of fetal hearts with anti-C5 at E10.5, E14.5, and E18.5 (Left), and the relative IOD of C5 (Right) (n = 4). Data are expressed as means ± SEM; *p < 0.05, **p < 0.01, ***p < 0.001 versus the vehicle control.

cell death, and vascular remodeling,[56,57] which were consistent with our findings.

Based on the above KEGG analysis, there were 10, 8, and 7 DEGs involved in the *Complement and coagulation cascades* pathway at E10.5, E14.5, and E18.5, respectively (Figure 5A). qPCR and IHC analyses further validated the expression of these DEGs and showed that coagulation-related genes continued to change following maternal $PM_{2.5}$ exposure (Figures 5B,C and S5), while complement-related genes were significantly upregulated only at E18.5 (Figure 5D,E). Consistently, the level of MAC, an effector molecule produced by the activated complement system, increased significantly at E18.5 following maternal $PM_{2.5}$ exposure (Figure S6A). In addition, the expression of key inflammatory genes and chemokines was significantly upregulated at E18.5 (Figure S6B). Then, we further comprehensively examined the role of these genes in the complement and coagulation cascades over successive developmental time series (Figure 6). Surprisingly, as the development progressed, the DEGs gradually shifted from coagulation regulation in midgestation to complement regulation in late gestation, reflecting a temporal activation of these pathways. Specifically, maternal $PM_{2.5}$ exposure initially activated the intrinsic pathway of the coagulation cascade in fetal hearts at E10.5; subsequently, the exposure promoted the

https://doi.org/10.1021/acs.est.4c11407
Environ. Sci. Technol. XXXX, XXX, XXX−XXX

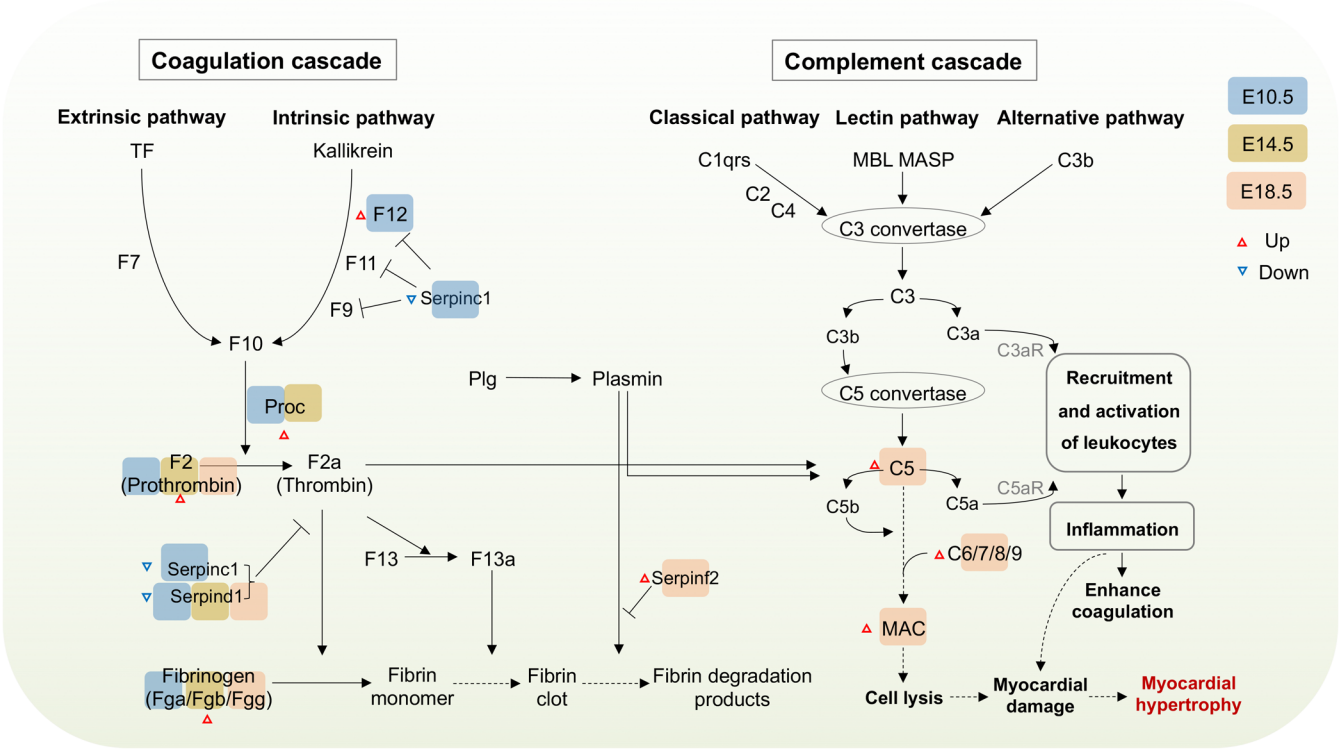

Figure 6. Crosstalk between the coagulation system and the complement system in developing fetal hearts following maternal $PM_{2.5}$ exposure. (Differentially expressed genes at E10.5, E14.5, and E18.5 are represented by blue, yellow, and flesh-pink backgrounds, respectively, with up-regulated genes marked by red triangles and down-regulated genes marked by blue triangles).

conversion of prothrombin to thrombin and drove fibrin production at E14.5; and finally, thrombin activated the complement cascade by targeting C5, resulting in myocardial injury at E18.5. Activation of the complement and coagulation systems can produce inflammatory mediators, such as C3a and C5a, which activate a variety of intracellular signaling pathways and bind to the promoter regions of myosin genes to stimulate myosin transcription.[58] In addition, the interaction between the complement and coagulation cascades generates the MAC, which directly causes insult to the cell membrane of cardiomyocytes and activates intracellular stress-related signaling pathways (e.g., the p38 MAPK signaling pathway) to regulate the expression of myosin genes, ultimately leading to myocardial hypertrophy.[59,60]

Furthermore, to compensate for the limitation of relying only on transcriptome analysis, we designed inhibition studies using recombinant hirudin as a thrombin inhibitor. Hirudin is a highly specific inhibitor of thrombin, which be a superior antithrombotic drug.[61−63] The findings consistent with our previous results, maternal $PM_{2.5}$ exposure caused abnormal left ventricular (LV) function and cardiac structure in male and female offspring, whereas recombinant hirudin treatment significantly attenuated the $PM_{2.5}$-induced adverse effects (Figure S7). Meanwhile, H&E staining and qRT-PCR results also confirmed the ameliorative effects of recombinant hirudin on $PM_{2.5}$-induced cardiac hypertrophy and abnormal activation of complement coagulation cascade (Figure S8). These results directly validate the critical role of complement and coagulation cascades in cardiac developmental toxicity induced by $PM_{2.5}$ at a functional level, adding to the reliability and completeness of the study.

The study has some limitations due to geographical variations in $PM_{2.5}$ components. First, our previous study examined the concentrations of 31 inorganic elements and 15 polycyclic aromatic hydrocarbons (PAHs) in $PM_{2.5}$ samples collected during the winter heating season, which were used in this study.[19] And we should link these inorganic and organic components to the adverse outcomes and related biological processes. Second, we should systematically apply this time-series regulatory mechanism in cardiac development by integrating multiple technologies (e.g., joint multiomics analysis of spatial and protein transcriptomes, etc.), or investigate the potential roles of key time-series genes by gene editing technologies, such as CRISPR, promoting the clinical prevention and treatment of CHDs.

Taken together, maternal $PM_{2.5}$ exposure caused cardiac systolic and diastolic dysfunction, as well as concentric myocardial hypertrophy in fetuses and neonates. E18.5 could be considered the critical window for structural changes and elevated myosin gene expression relevant to cardiac contraction. Mechanistically, the exposure initiated persistent crosstalk between the coagulation and complement systems, thereby triggering cellular inflammation and lysis, upregulating myosin genes, and ultimately contributing to compensatory cardiac hypertrophy and compromised cardiac function. Our findings give novel insights into CHD risks based on developmental origin in $PM_{2.5}$-polluted areas and provide potential cellular/molecular targets for control and prevention.

4. ENVIRONMENTAL IMPLICATIONS

Increasing epidemiological evidence indicates a close relationship between ambient $PM_{2.5}$ exposure and an increased risk of CHDs. However, the developmental origins as well as underlying mechanisms remain elusive. This study combines animal exposure, critical window identification and toxico-

https://doi.org/10.1021/acs.est.4c11407
Environ. Sci. Technol. XXXX, XXX, XXX−XXX

logical mechanisms to provide experimental data for not only CHD progression from environmental relevant level but also molecular targets for risk prevention; and further offers new insights for local governments and municipalities to mitigate regional ambient pollution and reduce health burden on children.

■ ASSOCIATED CONTENT

Supporting Information

The Supporting Information is available free of charge at https://pubs.acs.org/doi/10.1021/acs.est.4c11407.

Additional experimental details and results: specific method of Hematoxylin and Eosin (H&E) and Wheat Germ Agglutinin (WGA); effects of maternal $PM_{2.5}$ exposure on cardiac function and structural alterations; information on RNA-Seq profiles of critical cardiac developmental windows and so on (PDF)

■ AUTHOR INFORMATION

Corresponding Authors

Guangke Li − *Shanxi Key Laboratory of Coal-Based Emerging Pollutant Identification and Risk Control, Research Center of Environment and Health, College of Environment and Resource, Shanxi University, Shanxi 030006, P. R. China*; Email: liguangke@sxu.edu

Nan Sang − *Shanxi Key Laboratory of Coal-Based Emerging Pollutant Identification and Risk Control, Research Center of Environment and Health, College of Environment and Resource, Shanxi University, Shanxi 030006, P. R. China*; orcid.org/0000-0002-2433-3200; Email: sangnan@sxu.edu.cn

Authors

Yuqiong Guo − *Shanxi Key Laboratory of Coal-Based Emerging Pollutant Identification and Risk Control, Research Center of Environment and Health, College of Environment and Resource, Shanxi University, Shanxi 030006, P. R. China*

Sican Niu − *Shanxi Key Laboratory of Coal-Based Emerging Pollutant Identification and Risk Control, Research Center of Environment and Health, College of Environment and Resource, Shanxi University, Shanxi 030006, P. R. China*

Yingying Zhang − *Shanxi Key Laboratory of Coal-Based Emerging Pollutant Identification and Risk Control, Research Center of Environment and Health, College of Environment and Resource, Shanxi University, Shanxi 030006, P. R. China*

Wei Yan − *Xuzhou Engineering Research Center of Medical Genetics and Transformation, Key Laboratory of Genetic Foundation and Clinical Application, Department of Genetics, Xuzhou Medical University, Xuzhou, Jiangsu 221004, P. R. China*

Shaoyang Ji − *Shanxi Key Laboratory of Coal-Based Emerging Pollutant Identification and Risk Control, Research Center of Environment and Health, College of Environment and Resource, Shanxi University, Shanxi 030006, P. R. China*

Li Ma − *Shanxi Key Laboratory of Coal-Based Emerging Pollutant Identification and Risk Control, Research Center of Environment and Health, College of Environment and Resource, Shanxi University, Shanxi 030006, P. R. China*

Complete contact information is available at: https://pubs.acs.org/10.1021/acs.est.4c11407

Notes

The authors declare no competing financial interest.

■ ACKNOWLEDGMENTS

This study was supported by the National Natural Science Foundation of China (U23A20103, 22276117) and the Special Fund for Scientific and Technological Innovation Talent Teams of Shanxi Province (No. 202204051002024).

■ REFERENCES

(1) Triedman, J. K.; Newburger, J. W. Trends in Congenital Heart Disease. *Circulation* **2016**, *133* (25), 2716−2733.

(2) Sugimoto, M.; Kuwata, S.; Kurishima, C.; Kim, J. H.; Iwamoto, Y.; Senzaki, H. Cardiac Biomarkers in Children with Congenital Heart Disease. *World J. Pediatr.* **2015**, *11* (4), 309−315.

(3) Van Der Linde, D.; Konings, E. E. M.; Slager, M. A.; Witsenburg, M.; Helbing, W. A.; Takkenberg, J. J. M.; Roos-Hesselink, J. W. Birth Prevalence of Congenital Heart Disease Worldwide: A Systematic Review and Meta-Analysis. *J. Am. Coll. Cardiol.* **2011**, *58* (21), 2241−2247.

(4) Boyd, R.; McMullen, H.; Beqaj, H.; Kalfa, D. Environmental Exposures and Congenital Heart Disease. *Pediatrics* **2022**, *149* (1), No. e2021052151.

(5) Luo, X.; Liu, L.; Rong, H.; Liu, X.; Yang, L.; Li, N.; Shi, H. ENU-Based Dominant Genetic Screen Identifies Contractile and Neuronal Gene Mutations in Congenital Heart Disease. *Genome Med.* **2024**, *16* (1), No. 97.

(6) Zimmerman, M. S.; Smith, A. G. C.; Sable, C. A.; Echko, M. M.; Wilner, L. B.; Olsen, H. E.; Atalay, H. T.; Awasthi, A.; Bhutta, Z. A.; Boucher, J. L. A.; Castro, F.; Cortesi, P. A.; Dubey, M.; Fischer, F.; Hamidi, S.; Hay, S. I.; Hoang, C. L.; Hugo-Hamman, C.; Jenkins, K. J.; Kar, A.; Khalil, I. A.; Kumar, R. K.; Kwan, G. F.; Mengistu, D. T.; Mokdad, A. H.; Naghavi, M.; Negesa, L.; Negoi, I.; Negoi, R. I.; Nguyen, C. T.; Nguyen, H. L. T.; Nguyen, L. H.; Nguyen, S. H.; Nguyen, T. H.; Nixon, M. R.; Noubiap, J. J.; Patel, S.; Peprah, E. K.; Reiner, R. C.; Roth, G. A.; Temsah, M. H.; Tovani-Palone, M. R.; Towbin, J. A.; Tran, B. X.; Tran, T. T.; Truong, N. T.; Vos, T.; Vosoughi, K.; Weintraub, R. G.; Weldegwergs, K. G.; Zaidi, Z.; Zheleva, B.; Zuhlke, L.; Murray, C. J. L.; Martin, G. R.; Kassebaum, N. J. Global, Regional, and National Burden of Congenital Heart Disease, 1990−2017: A Systematic Analysis for the Global Burden of Disease Study 2017. *Lancet Child Adolesc. Health* **2020**, *4* (3), 185−200.

(7) Zhang, B.; Liang, S.; Zhao, J.; Qian, Z.; Bassig, B. A.; Yang, R.; Zhang, Y.; Hu, K.; Xu, S.; Zheng, T.; Yang, S. Maternal Exposure to Air Pollutant $PM_{2.5}$ and PM_{10} during Pregnancy and Risk of Congenital Heart Defects. *J. Exposure Sci. Environ. Epidemiol.* **2016**, *26* (4), 422−427.

(8) Hall, K. C.; Robinson, J. C.; Cooke, W. H.; Parnell, A. S.; Zhang, L.; Northington, L. Relationship between Environmental Air Quality and Congenital Heart Defects. *Nurs. Res.* **2022**, *71* (4), 266−274.

(9) Buteau, S.; Veira, P.; Bilodeau-Bertrand, M.; Auger, N. Association between First Trimester Exposure to Ambient $PM_{2.5}$ and NO_2 and Congenital Heart Defects: A Population-Based Cohort Study of 1,342,198 Live Births in Canada. *Environ. Health Perspect.* **2023**, *131* (6), No. 607009.

(10) Yuan, X.; Liang, F.; Zhu, J.; Huang, K.; Dai, L.; Li, X.; Wang, Y.; Li, Q.; Lu, X.; Huang, J.; Liao, L.; Liu, Y.; Gu, D.; Liu, H.; Liu, F. Maternal Exposure to $PM_{2.5}$ and the Risk of Congenital Heart Defects in 1.4 Million Births: A Nationwide Surveillance-Based Study. *Circulation* **2023**, *147* (7), 565−574.

(11) Warren, J. L.; Stingone, J. A.; Herring, A. H.; Luben, T. J.; Fuentes, M.; Aylsworth, A. S.; Langlois, P. H.; Botto, L. D.; Correa, A.; Olshan, A. F. Bayesian Multinomial Probit Modeling of Daily Windows of Susceptibility for Maternal $PM_{2.5}$ Exposure and Congenital Heart Defects. *Stat. Med.* **2016**, *35* (16), 2786−2801.

(12) Wang, G.; Wang, B.; Yang, P. Epigenetics in Congenital Heart Disease. *J. Am. Heart Assoc.* **2022**, *11* (7), No. e025163.

(13) Zaidi, S.; Brueckner, M. Genetics and Genomics of Congenital Heart Disease. *Circ. Res.* **2017**, *120* (6), 923−940.
(14) Yue, Y.; Zong, W.; Li, X.; Li, J.; Zhang, Y.; Wu, R.; Liu, Y.; Cui, J.; Wang, Q.; Bian, Y.; Yu, X.; Liu, Y.; Tan, G.; Zhang, Y.; Zhao, G.; Zhou, B.; Chen, L.; Xiao, W.; Cheng, H.; He, A. Long-Term, in Toto Live Imaging of Cardiomyocyte Behaviour during Mouse Ventricle Chamber Formation at Single-Cell Resolution. *Nat. Cell Biol.* **2020**, *22* (3), 332−340.
(15) Cui, Y.; Zheng, Y.; Liu, X.; Yan, L.; Fan, X.; Yong, J.; Hu, Y.; Dong, J.; Li, Q.; Wu, X.; Gao, S.; Li, J.; Wen, L.; Qiao, J.; Tang, F. Single-Cell Transcriptome Analysis Maps the Developmental Track of the Human Heart. *Cell Rep.* **2019**, *26* (7), 1934−1950.
(16) Tanwar, V.; Gorr, M. W.; Velten, M.; Eichenseer, C. M.; Long, V. P.; Bonilla, I. M.; Shettigar, V.; Ziolo, M. T.; Davis, J. P.; Baine, S. H.; Carnes, C. A.; Wold, L. E. In Utero Particulate Matter Exposure Produces Heart Failure, Electrical Remodeling, and Epigenetic Changes at Adulthood. *J. Am. Heart Assoc.* **2017**, *6* (4), No. e005796.
(17) Tanwar, V.; Adelstein, J. M.; Grimmer, J. A.; Youtz, D. J.; Sugar, B. P.; Wold, L. E. $PM_{2.5}$ Exposure in Utero Contributes to Neonatal Cardiac Dysfunction in Mice. *Environ. Pollut.* **2017**, *230*, 116−124.
(18) Ku, T.; Li, B.; Gao, R.; Zhang, Y.; Yan, W.; Ji, X.; Li, G.; Sang, N. NF-KB-Regulated MicroRNA-574−5p Underlies Synaptic and Cognitive Impairment in Response to Atmospheric $PM_{2.5}$ Aspiration. *Part. Fibre Toxicol.* **2017**, *14* (1), No. 34.
(19) Hou, Y.; Yan, W.; Guo, L.; Li, G.; Sang, N. Prenatal $PM_{2.5}$ Exposure Impairs Spatial Learning and Memory in Male Mice Offspring: From Transcriptional Regulation to Neuronal Morphogenesis. *Part. Fibre Toxicol.* **2023**, *20* (1), No. 13.
(20) Li, D.; Gao, R.; Qin, L.; Yue, H.; Sang, N. New Insights into Prenatal NO_2 Exposure and Behavioral Abnormalities in Male Offspring: Disturbed Serotonin Metabolism and Delayed Oligodendrocyte Development. *Environ. Sci. Technol.* **2022**, *56* (16), 11536−11546.
(21) Ji, S.; Guo, Y.; Li, G.; Sang, N. NO_2 Exposure Contributes to Cardiac Hypertrophy in Male Mice through Apoptosis Signaling Pathways. *Chemosphere* **2022**, *309*, No. 136576.
(22) Knutson, O. C. A.; Luben, T. J.; Stingone, J. A.; Engel, L. S.; Martin, C. L.; Olshan, A. F. Racial Disparities in Maternal Exposure to Ambient Air Pollution During Pregnancy and Prevalence of Congenital Heart Defects. *Am. J. Epidemiol.* **2025**, *194*, 709−721, DOI: 10.1093/aje/kwae253.
(23) Sun, J.; Wang, J.; Yang, J.; Shi, X.; Li, S.; Cheng, J.; Chen, S.; Sun, K.; Wu, Y. Association between Maternal Exposure to Indoor Air Pollution and Offspring Congenital Heart Disease: A Case-Control Study in East China. *BMC Public Health* **2022**, *22* (1), No. 767.
(24) Agay-Shay, K.; Friger, M.; Linn, S.; Peled, A.; Amitai, Y.; Peretz, C. Air Pollution and Congenital Heart Defects. *Environ. Res.* **2013**, *124*, 28−34.
(25) Baudouy, D.; Michiels, J. F.; Vukolic, A.; Wagner, K. D.; Wagner, N. Echocardiographic and Histological Examination of Cardiac Morphology in the Mouse. *J. Visualized Exp.* **2017**, *26* (128), No. 55843.
(26) Costantino, S.; Ambrosini, S.; Mohammed, S. A.; Gorica, E.; Akhmedov, A.; Cosentino, F.; Ruschitzka, F.; Hamdani, N.; Paneni, F. A chromatin mark by SETD7 regulates myocardial inflammation in obesity-related heart failure with preserved ejection fraction. *Eur. Heart J.* **2022**, *43*, No. ehac544.2883.
(27) Jost, K.; Datta, A. N.; Frey, U. P.; Suki, B.; Schulzke, S. M. Heart Rate Fluctuation after Birth Predicts Subsequent Cardiorespiratory Stability in Preterm Infants. *Pediatr. Res.* **2019**, *86* (3), 348−354.
(28) Peterzan, M. A.; Lygate, C. A.; Neubauer, S.; Rider, O. J. Metabolic Remodeling in Hypertrophied and Failing Myocardium: A Review. *Am. J. Physiol-Heart Circ. Physiol.* **2017**, *313*, 597−616.
(29) Guo, Y.; Pu, W. T. Cardiomyocyte Maturation: New Phase in Development. *Circ. Res.* **2020**, *126*, 1086−1106.
(30) Sánchez-Gómez, M. C.; García-Mejía, K. A.; Pérez-Díaz Conti, M.; Díaz-Rosas, G.; Palma-Lara, I.; Sánchez-Urbina, R.; Klünder-Klünder, M.; Botello-Flores, J. A.; Balderrábano- Saucedo, N. A.; Contreras-Ramos, A. MicroRNAs Association in the Cardiac Hypertrophy Secondary to Complex Congenital Heart Disease in Children. *Pediatr. Cardiol.* **2017**, *38* (5), 991−1003.
(31) Yamazaki, T.; Komuro, I.; Yazaki, Y. Role of the Renin-Angiotensin System in Cardiac Hypertrophy. *Am. J. Cardiol.* **1999**, *83*, 53−57.
(32) Goodson, J. M.; MacDonald, J. W.; Bammler, T. K.; Chien, W. M.; Chin, M. T. In Utero Exposure to Diesel Exhaust Is Associated with Alterations in Neonatal Cardiomyocyte Transcription, DNA Methylation and Metabolic Perturbation. *Part. Fibre Toxicol.* **2019**, *16* (1), No. 17.
(33) Hoffman, D. J.; Reynolds, R. M.; Hardy, D. B. Developmental Origins of Health and Disease: Current Knowledge and Potential Mechanisms. *Nutr. Rev.* **2017**, *75* (12), 951−970.
(34) Toepfer, C. N.; Garfinkel, A. C.; Venturini, G.; Wakimoto, H.; Repetti, G.; Alamo, L.; Sharma, A.; Agarwal, R.; Ewoldt, J. F.; Cloonan, P.; Letendre, J.; Lun, M.; Olivotto, I.; Colan, S.; Ashley, E.; Jacoby, D.; Michels, M.; Redwood, C. S.; Watkins, H. C.; Day, S. M.; Staples, J. F.; Padrón, R.; Chopra, A.; Ho, C. Y.; Chen, C. S.; Pereira, A. C.; Seidman, J. G.; Seidman, C. E. Myosin Sequestration Regulates Sarcomere Function, Cardiomyocyte Energetics, and Metabolism, Informing the Pathogenesis of Hypertrophic Cardiomyopathy. *Circulation* **2020**, *141* (10), 828−842.
(35) Park, A. C.; Mann, D. L. The Pathobiology of Myocardial Recovery and Remission: From Animal Models to Clinical Observations in Heart Failure Patients. *Methodist DeBakey Cardiovasc. J.* **2024**, *20* (4), 16−30.
(36) Akazawa, H.; Komuro, I. Roles of Cardiac Transcription Factors in Cardiac Hypertrophy. *Circ. Res.* **2003**, *92* (10), 1079−1088.
(37) Gaggin, H. K.; Januzzi, J. L. Biomarkers and Diagnostics in Heart Failure. *Biochim. Biophys. Acta, Mol. Basis Dis.* **2013**, *1832* (12), 2442−2450.
(38) A, P.; Varghese, M. V.; Abhilash, S.; Salin Raj, P.; Mathew, A. K.; Nair, A.; Nair, R. H.; R, K. G. Polyphenol Rich Ethanolic Extract from Boerhavia Diffusa L. Mitigates Angiotensin II Induced Cardiac Hypertrophy and Fibrosis in Rats. *Biomed. Pharmacother.* **2017**, *87*, 427−436.
(39) Nadar, S. K.; Lip, G. Y. H. The Heart in Hypertension. *J. Hum. Hypertens.* **2021**, *35* (5), 383−386.
(40) Szedlak, P.; Steele, D. S.; Hopkins, P. M. Cardiac Muscle Physiology. *BJA Educ.* **2023**, *23* (9), 350−357.
(41) Muir, W. W.; Hamlin, R. L. Myocardial Contractility: Historical and Contemporary Considerations. *Front. Physiol.* **2020**, *11*, No. 222.
(42) Daniels, M. J.; Fusi, L.; Semsarian, C.; Naidu, S. S. Myosin Modulation in Hypertrophic Cardiomyopathy and Systolic Heart Failure: Getting Inside the Engine. *Circulation* **2021**, *144* (10), 759−762.
(43) Hartman, J. J.; Hwee, D. T.; Robert-Paganin, J.; Chuang, C.; Chin, E. R.; Edell, S.; Lee, K. H.; Madhvani, R.; Paliwal, P.; Pernier, J.; Sarkar, S. S.; Schaletzky, J.; Schauer, K.; Taheri, K. D.; Wang, J.; Wehri, E.; Wu, Y.; Houdusse, A.; Morgan, B. P.; Malik, F. I. Aficamten Is a Small-Molecule Cardiac Myosin Inhibitor Designed to Treat Hypertrophic Cardiomyopathy. *Nat. Cardiovasc. Res.* **2024**, *3* (8), 1003−1016.
(44) England, J.; Loughna, S. Heavy and Light Roles: Myosin in the Morphogenesis of the Heart. *Cell. Mol. Life Sci.* **2013**, *70* (7), 1221−1239.
(45) Toepfer, C. N.; Garfinkel, A. C.; Venturini, G.; Wakimoto, H.; Repetti, G.; Alamo, L.; Sharma, A.; Agarwal, R.; Ewoldt, J. F.; Cloonan, P.; Letendre, J.; Lun, M.; Olivotto, I.; Colan, S.; Ashley, E.; Jacoby, D.; Michels, M.; Redwood, C. S.; Watkins, H. C.; Day, S. M.; Staples, J. F.; Padrón, R.; Chopra, A.; Ho, C. Y.; Chen, C. S.; Pereira, A. C.; Seidman, J. G.; Seidman, C. E. Myosin Sequestration Regulates Sarcomere Function, Cardiomyocyte Energetics, and Metabolism, Informing the Pathogenesis of Hypertrophic Cardiomyopathy. *Circulation* **2020**, *141* (10), 828−842.
(46) Yeh, H.; Chang, Y.-M.; Chang, Y.-W.; Lu, M.-Y. J.; Chen, Y.-H.; Lee, C.-C.; Chen, C.-C. Multiomic Analyses Reveal Enriched Glycolytic Processes in β-Myosin Heavy Chain-Expressed Cardio-

https://doi.org/10.1021/acs.est.4c11407
Environ. Sci. Technol. XXXX, XXX, XXX−XXX

myocytes in Early Cardiac Hypertrophy. *J. Mol. Cell Cardiol. Plus* **2022**, *1*, No. 100011.
(47) Desai, M. Y.; Owens, A.; Geske, J. B.; Wolski, K.; Naidu, S. S.; Smedira, N. G.; Cremer, P. C.; Schaff, H.; McErlean, E.; Sewell, C.; Li, W.; Sterling, L.; Lampl, K.; Edelberg, J. M.; Sehnert, A. J.; Nissen, S. E. Myosin Inhibition in Patients with Obstructive Hypertrophic Cardiomyopathy Referred for Septal Reduction Therapy. *J. Am. Coll. Cardiol.* **2022**, *80* (2), 95−108.
(48) Hernandez, S. G.; Romero, D. L. H. R.; Fernandez, X.; Gomez, M. V.; Varela, L. C.; Deben, R. P.; Rebolo, P.; Verdes, A. S.; Cardenas, I.; Ortiz-Genga, M.; Salamanca, A. A.; Barbeito, M. P.; Diaz, I. G.; Flores, M. S.; Ochoa, J. P. Narrowing Beta-Myosin Hot Spots in Its Association with Hypertrophic Cardiomyopathy. *Eur. Heart J.* **2022**, *43*, No. ehac544.1740.
(49) Nag, S.; Trivedi, D. V.; Sarkar, S. S.; Adhikari, A. S.; Sunitha, M. S.; Sutton, S.; Ruppel, K. M.; Spudich, J. A. The Myosin Mesa and the Basis of Hypercontractility Caused by Hypertrophic Cardiomyopathy Mutations. *Nat. Struct. Mol. Biol.* **2017**, *24* (6), 525−533.
(50) Adhikari, A. S.; Trivedi, D. V.; Sarkar, S. S.; Song, D.; Kooiker, K. B.; Bernstein, D.; Spudich, J. A.; Ruppel, K. M. *β*-Cardiac Myosin Hypertrophic Cardiomyopathy Mutations Release Sequestered Heads and Increase Enzymatic Activity. *Nat. Commun.* **2019**, *10* (1), No. 2685.
(51) Sun, K.; Liu, X.; Lan, X. A Single-Cell Atlas of Chromatin Accessibility in Mouse Organogenesis. *Nat. Cell Biol.* **2024**, *26* (7), 1200−1211.
(52) Dzik, S. Complement and Coagulation: Cross Talk Through Time. *Transfus. Med. Rev.* **2019**, *33* (4), 199−206.
(53) Markiewski, M. M.; Nilsson, B.; Nilsson Ekdahl, K.; Mollnes, T. E.; Lambris, J. D. Complement and Coagulation: Strangers or Partners in Crime? *Trends Immunol.* **2007**, *28* (4), 184−192.
(54) Foley, J. H.; Conway, E. M. Cross Talk Pathways between Coagulation and Inflammation. *Circ. Res.* **2016**, *118* (9), 1392−1408.
(55) Jin, X.; Ma, Q.; Sun, Z.; Yang, X.; Zhou, Q.; Qu, G.; Liu, Q.; Liao, C.; Li, Z.; Jiang, G. Airborne Fine Particles Induce Hematological Effects through Regulating the Crosstalk of the Kallikrein-Kinin, Complement, and Coagulation Systems. *Environ. Sci. Technol.* **2019**, *53* (5), 2840−2851.
(56) Youssef, L.; Miranda, J.; Blasco, M.; Paules, C.; Crovetto, F.; Palomo, M.; Torramade-Moix, S.; García-Calderó, H.; Tura-Ceide, O.; Dantas, A. P.; Hernandez-Gea, V.; Herrero, P.; Canela, N.; Campistol, J. M.; Garcia-Pagan, J. C.; Diaz-Ricart, M.; Gratacos, E.; Crispi, F. Complement and Coagulation Cascades Activation Is the Main Pathophysiological Pathway in Early-Onset Severe Preeclampsia Revealed by Maternal Proteomics. *Sci. Rep.* **2021**, *11* (1), No. 3048.
(57) Reis, E. S.; Mastellos, D. C.; Hajishengallis, G.; Lambris, J. D. New Insights into the Immune Functions of Complement. *Nat. Rev. Immunol.* **2019**, *19* (8), 503−516.
(58) Chimenti, M. S.; Ballanti, E.; Triggianese, P.; Perricone, R. Vasculitides and the Complement System: A Comprehensive Review. *Clin Rev. Allergy Immunol.* **2015**, *49* (3), 333−346.
(59) Saucerman, J. J.; Tan, P. M.; Buchholz, K. S.; McCulloch, A. D.; Omens, J. H. Mechanical Regulation of Gene Expression in Cardiac Myocytes and Fibroblasts. *Nat. Rev. Cardiol.* **2019**, *16* (6), 361−378.
(60) Zhang, Z. Association of C5a/C5aR Pathway to Activate ERK1/2 and P38 MAPK in Acute Kidney Injury − a Mouse Model. *Rev. Rom. Med. Lab.* **2022**, *30* (1), 31−40.
(61) Verstraete, M.; Nurmohamed, M.; Kienast, J.; Siebeck, M.; Silling-Engelhardt, G.; Büller, H.; Hoet, B.; Bichler, J.; Close, P. Biologic Effects of Recombinant Hirudin (CGP 39393) In Human Volunteers. European Hirudin in Thrombosis Group. *J. Am. Coll. Cardiol.* **1993**, *22* (4), 1080−1088.
(62) Lee, R. H.; Kawano, T.; Bharathi, V.; Martinez, D.; Cowley, D. O.; Grover, S. P.; Mackman, N.; Bergmeier, W.; Antoniak, S. Investigating the Roles of Platelet PAR4 in Hemostasis, Thrombosis and Viral Infection Using a Newly Generated PAR4 Floxed Mouse. *Blood* **2021**, *138*, No. 151121.
(63) Ying-Xin, G.; Yin, G.; Li, J.; Xiao, H. Effects of Natural and Recombinant Hirudin on Superoxide Dismutase, Malondialdehyde and Endothelin Levels in A Random Pattern Skin Flap Model. *J. Hand Surg. (Eur. Vol.)* **2012**, *37* (1), 42−49.

https://doi.org/10.1021/acs.est.4c11407
Environ. Sci. Technol. XXXX, XXX, XXX−XXX